A simple genetic architecture and low constraint allows rapid floral evolution in a diverse and recently radiating plant genus

Jamie L. Kostyun[1,2*], Matthew J.S. Gibson[1], Christian M. King[1,3], and Leonie C. Moyle[1]

[1] Department of Biology, Indiana University, Bloomington, IN 47405

[2] Department of Plant Biology, The University of Vermont, Burlington, VT 05405

[3] Department of Evolution, Ecology and Organismal Biology, The Ohio State University, Columbus, OH 43210

* Corresponding author: Jamie.Kostyun@uvm.edu, Tel: 802-656-7670

Word count: Summary (200), Introduction (1185), Materials and Methods (1576), Results (1010), Discussion (1821), Acknowledgements (79), Total Main Text (5706), Figures (4, all in color), Tables (2), Supplementary Documents (8 Figures, 7 Tables).

Summary

- Genetic correlations among different components of phenotypes, especially resulting from pleiotropy, can constrain (antagonistic) or facilitate (adaptive) trait evolution. These factors could especially influence the evolution of traits that are functionally integrated, such as those comprising the flower. Indeed, pleiotropy is proposed as a main driver of repeated convergent trait transitions, including the evolution of phenotypically-similar pollinator syndromes.
- We assessed the role of pleiotropy in the differentiation of floral and other reproductive traits between two species—*Jaltomata sinuosa* and *J. umbellata* (Solanaceae)—that have divergent suites of floral traits consistent with bee- and hummingbird-pollination, respectively. To do so, we generated a hybrid population and examined the genetic architecture (trait segregation and QTL distribution) underlying 25 floral and fertility traits.
- We found that most traits had a relatively simple genetic basis (few, predominantly additive, QTL of moderate to large effect), as well as little evidence of antagonistic pleiotropy (few trait correlations and QTL co-localization, particularly between traits of different classes). However, we did detect a potential case of adaptive pleiotropy among floral size and nectar traits.
- These mechanisms may have facilitated the rapid floral trait evolution observed within *Jaltomata*, and may be a common component of rapid phenotypic change more broadly.

Key Words: floral evolution, genetic co-variation, *Jaltomata*, pleiotropy, Solanaceae, QTL co-localization, QTL mapping

48 **Introduction**

49 One feature of phenotypic evolution is the broad variation in observed rates of
50 trait change, both among traits within a single lineage and among lineages. How quickly
51 phenotypes evolve and in what direction, depends not only on their genetic basis--both
52 the number and effect size of causal loci--and the intensity and nature of selection acting
53 upon them, but also on their associations with other traits. Because of genetic covariance,
54 developmental and phylogenetic constraints, and/or correlated selection pressures
55 (Agrawal and Stinchombe 2009), phenotypic traits often do not evolve independently
56 from one another. Among these causal mechanisms, strong genetic covariance arises
57 either because different traits have a shared genetic basis (pleiotropy) or because they are
58 based on genes that are physically adjacent and therefore often co-inherited (via linkage).
59 Strong pleiotropy is often proposed to constrain phenotypic evolution by preventing
60 correlated traits from moving efficiently towards their own (different) fitness optima
61 (antagonistic pleiotropy). However, such shared genetic control may also promote
62 phenotypic change if covariation is aligned in the direction of selection (adaptive
63 pleiotropy) (Agrawal and Stinchombe 2009; Wagner and Zhang 2011; Smith 2016).
64 Nonetheless, despite some detailed studies (e.g. Ettensohn 2013; Shrestha et al. 2014;
65 Manceau et al. 2011; Xu and Schluter 2015), the genetic architecture of many
66 ecologically important traits remains unclear, including the prevalence of strong genetic
67 associations that could shape the course of phenotypic evolution.

68 How shared architecture influences phenotypic change is especially relevant for
69 suites of traits that are functionally integrated (Armbruster et al. 2014) -- such as the
70 angiosperm flower (Armbruster et al. 2009) -- because the magnitude and direction of

pleiotropy will directly shape if and how these co-varying traits respond to selection. Further, because pleiotropy can constrain or favor particular developmental trajectories, it is often proposed to be a main driver of convergent transitions of integrated traits in different lineages (Preston et al. 2011; Smith 2016). The flower is an especially promising model for assessing the role of pleiotropy in shaping phenotypic evolution. Because flowers mediate fitness through their critical reproductive role, their constituent traits (i.e. reproductive structures, perianth, and other attraction/reward features) are often highly functionally integrated (Conner 2002; Armbruster et al. 2009). Moreover, repeated transitions of phenotypically similar or convergent suites of floral traits have been identified both within and across groups (Fenster et al. 2004; Goodwillie et al. 2010; Wessinger et al. 2016). For example, multiple parallel shifts from bee-pollination to hummingbird-pollination are associated with parallel transitions to flowers with red petals, large amounts of dilute nectar, and narrow corolla tubes within *Penstemon* (Wessinger et al. 2016); similarly, the evolution of the 'selfing syndrome' (i.e. reduced overall size, herkogamy, and floral rewards) often accompanies transitions from outcrossing to predominantly selfing mating systems, and has been documented in multiple lineages (Stebbins 1974; Goodwillie et al. 2010). Such patterns provide an opportunity to assess the relative frequency of adaptive vs. antagonistic pleiotropy in shaping these repeated trait combinations, within a comparative phylogenetic context.

In addition to these ecological and evolutionary features, the known genetic and molecular bases of floral development (Rijpkema et al. 2006; Smaczniak et al. 2012) themselves suggest that pleiotropy might be a key component shaping floral phenotypic change, as well as provide a functionally-informed framework for identifying how

94 changes in these mechanisms can contribute to the diversification of floral traits. Under
95 the ABC(DE) model of floral development, the combinatorial action of different gene
96 products -- primarily different MADS-box transcription factors -- control transitions to
97 flowering and the specification of floral organ identities and organ maturation, by
98 promoting or repressing different downstream targets (reviewed in O'Maoileidigh et al.
99 2014; Bartlett 2017). This combinatorial function, and the ability to regulate shared or
100 partially shared downstream targets, provides a potential mechanistic explanation for
101 strong pleiotropy among floral traits. Moreover, several key regulators of floral
102 development also function during fruit and seed production (Smaczniak et al. 2012;
103 O'Maoileidigh et al. 2014); such correlated effects on fertility traits are another potential
104 way that pleiotropy could shape floral phenotypic evolution.

105 Several empirical approaches have been taken to assess the genetic architecture
106 underlying floral trait specification and evolution, and to evaluate the strength and
107 direction of pleiotropy. Classical quantitative genetic analyses have revealed varying
108 degrees of genetic covariance among floral traits (Gottlieb 1984; Conner et al. 2014),
109 while numerous QTL (quantitative trait locus) mapping studies have found that loci for at
110 least some different floral traits appear to co-localize to the same genomic region(s)
111 (reviewed in Smith 2016). Interestingly, such studies have identified more putative cases
112 of adaptive pleiotropy (e.g. QTL affect more than one trait in the direction of parental
113 trait values) than antagonistic, suggesting that adaptive pleiotropy may be a common
114 mechanism contributing to rapid floral evolution. Because QTL generally span a genomic
115 region that contains more than one gene, such QTL co-localization is consistent with, but
116 not definitive evidence of, a role of pleiotropy in shaping floral trait co-variation (e.g. see

117 Hermann et al. 2013). Nonetheless, identifying strong trait correlations and/or QTL co-
118 localization represents a critical step in assessing how pervasive pleiotropy could be in
119 shaping floral trait evolution.

120 In this study, we examined phenotypic (co)variation among, and the genetic
121 architecture underlying, floral and other reproductive traits within a segregating hybrid
122 population derived from two *Jaltomata* (Solanaceae) species with divergent floral traits
123 (**Figure 1**). Despite only having diversified with the last 5 million years (Sarkinen et al.
124 2013; Wu et al. 2018), species of *Jaltomata* are highly phenotypically diverse, including
125 extensive variation in the size, shape, and color of floral traits that is absent among their
126 close relatives within *Solanum* and *Capsicum*. Indeed, phylogenetic analyses suggest
127 numerous transitions in floral traits within the genus, including several instances of
128 convergent evolution (Miller et al. 2011; Wu et al. 2018). Importantly, many of these
129 transitions appear to involve parallel changes in several different traits within a lineage
130 (e.g. from flat corollas with small amounts of lightly colored nectar to highly fused
131 corollas with large amounts of darkly colored nectar), suggesting either a shared genetic
132 basis and/or correlated selection (perhaps pollinator-mediated selection, Fenster et al.
133 2004) influences these trait associations.

134 Here, we identified QTL contributing to floral and other reproductive trait
135 variation within a recombinant population to: 1) examine the genetic architecture
136 underlying reproductive trait divergence; 2) assess the role of genetic linkage and/or
137 pleiotropy (via strong trait correlations and overlapping QTL) in floral trait (co)variation;
138 and 3) assess evidence for a shared genetic basis between different classes of floral trait
139 and other reproductive (specifically fertility) traits. We found evidence for a relatively

140 simple genetic basis underlying most of the examined traits, as well as positive
141 correlations and significant QTL co-localization among traits within each of three trait
142 classes (floral morphology, floral color, and fertility). Together, these features might
143 facilitate rapid changes in these traits. In comparison, we found few associations between
144 traits from different classes, and therefore little evidence for antagonistic pleiotropy
145 among these classes. One striking exception was an association between flower size and
146 nectar traits that acts in the direction exhibited by multiple species in the genus,
147 suggesting that this could instead be an instance of adaptive pleiotropy.
148

149 **MATERIALS AND METHODS**

150 ***Study system:*** *Jaltomata* (Schlechtendal; Solanaceae) is the sister genus to the
151 large and economically important *Solanum* (Olmstead et al. 2008; Sarkinen et al. 2013;
152 Wu et al. 2019), and includes approximately 60-80 species distributed from the
153 Southwestern United States to the Andean region of South America, in addition to several
154 species endemic to the Greater Antilles and the Galapagos Islands (Miller et al. 2011;
155 Mione et al. 2015). Species are highly phenotypically diverse and live in a variety of
156 habitats (e.g. tropical rainforests, rocky foothills, and *lomas* formations), despite their
157 recent divergence (<5MYA, Sarkinen et al. 2013).

158 Here, we focused on a closely related species pair, *J. sinuosa* and *J. umbellata*,
159 that differ in a suite of floral traits that is representative of major floral suites found in
160 other species throughout the genus (**Figure 1**; **Table S1**). *Jaltomata sinuosa* has large
161 rotate flowers with purple petals and a small amount of concentrated nectar (consistent
162 with bee pollination, Fenster et al. 2004), while *J. umbellata* has small short-tubular

163 flowers with white petals and a large amount of dilute, but dark red, nectar that is visible
164 through the corolla tube (consistent with hummingbird pollination, Fenster et al. 2004;
165 Kostyun and Moyle 2017; Mione et al. 2017). *Jaltomata sinuosa* is distributed along the
166 Andes in South America from Venezuela to Bolivia, while *J. umbellata* is restricted to
167 lomas formations along the Peruvian coast. Both species are self-compatible (Kostyun
168 and Moyle 2017; J.L. Kostyun and T. Mione, unpub.) and shrubby, but differ in leaf traits
169 such as overall size and shape, and type of trichomes. This species pair also has several
170 incomplete, intrinsic postzygotic reproductive barriers, including quantitatively reduced
171 fruit set and hybrid seed viability (Kostyun and Moyle 2017).

172 ***Generation of BC_1 population and plant cultivation:*** We developed a
173 segregating hybrid population by crossing *J. sinuosa* and *J. umbellata*. Viable F1
174 individuals in both directions of the cross produce flowers that are phenotypically
175 intermediate between the parental genotypes (**Figure 1**), and retain reduced but sufficient
176 levels of fertility when back-crossed to parents (Kostyun and Moyle 2017). Because we
177 were especially interested in the genetic basis of red nectar and a fused corolla tube
178 (exhibited by *J. umbellata* and F1s but not *J. sinuosa*), we generated the mapping
179 population by backcrossing a single *J. sinuosa* x *J. umbellata* F1 (as the ovule parent) to
180 the original parental *J. sinuosa* individual (as the pollen parent). BC1 individuals were
181 germinated in a growth chamber, and then moved to the Indiana University greenhouse
182 and grown under the same conditions as the parental and F1 individuals (16 hour light
183 cycle, watered twice daily, and fertilized weekly).

184 ***Trait measurements:*** We measured 25 floral and other reproductive traits within
185 our mapping population, F1, and parental genotypes (**Table 1; Table S2; Figure S1**).

186 Floral morphological traits were measured with hand-held calipers, and nectar volume
187 per flower was measured to the nearest 1 μL using a pipette. To reduce the potential
188 effect of daily environmental variation, nectar volume was always measured in the early
189 afternoon following watering.

190 Petal and nectar color were quantified using digital photography (Kendal et al.
191 2013; Garcia et al. 2014): dissected petals and nectar drops were photographed on a
192 standard background along with white and black color standards. Light conditions were
193 standardized for all images using RAW Therapee (RAW Therapee Development Team
194 2012), and color space attributes were measured in ImageJ (Schneider et al. 2012).
195 Because RGB color attributes are device-dependent (i.e. they can vary depending upon
196 the specific camera used), color values were also converted into device-independent
197 L*a*b color attributes, using the ImageJ Color Space Converter plugin (Schwartzwald
198 2012). For both petal and nectar color, this approach produced eight interrelated color
199 attributes: Intensity, Red, Green, Blue, Composite RGB, Lightness (L), 'a' color (ranges
200 from green to magenta), and 'b' color (ranges from cyan to yellow). Broadly, Intensity,
201 Red, Green, Blue, and Lightness convey information about color brightness, while
202 Composite RGB, 'a' color, and 'b' color convey information about hue.

203 We also measured nine fertility traits (**Table 1**) to assess the potential genetic
204 overlap between floral and other reproductive traits, as well as to examine the genetic
205 architecture underlying intrinsic postzygotic barriers between this species pair. Fruit and
206 seed related traits were measured on 2-6 crossed fruit per individual (depending on fruit
207 set). For F1 and BC1 individuals, crossed fruit were produced using pollen from the *J.*
208 *sinuosa* parental individual. To determine seed germination rates (following Farooq et al.

209 2005), we soaked 10 seeds per individual in 50% bleach for 30 minutes (to soften the
210 seed coat), rinsed thoroughly, and placed on moist paper within plastic germination
211 boxes. A week after sowing, seed coats were nicked slightly and seeds were given a drop
212 of 10 mM giberellic acid (Sigma) to break dormancy. We then scored germination every
213 2 weeks for 4 months. Pollen viability was estimated from three different flowers per
214 individual, using established methods (Jewell et al. 2012): Briefly, for each sample all
215 undehisced anthers from a flower were collected into an eppendorf tube containing
216 aniline blue histochemical stain, gently ground with a pestle to release pollen, and viable
217 pollen grains were counted under an EVOS FL Digital Inverted Fluorescence Microscope
218 (Fisher Scientific). From these data, we also calculated the proportion of viable pollen as
219 number of viable pollen grains/total pollen grains in the sample.

220 ***Statistical analyses on phenotypic data***: Following Shapiro-Wilk tests to assess
221 normality assumptions, we transformed traits that showed a skewed distribution and/or
222 significantly non-normal residuals. In particular, we arcsine transformed proportional
223 traits (proportion of corolla fusion, fruit set, and proportion of viable pollen), and log-
224 transformed inflorescence size, corolla fusion, petal length, style length, herkogamy,
225 nectar volume, all color attributes, and remaining fertility traits. Significant differences
226 between parental species for all traits were assessed by t-tests (**Table 1**). Distribution
227 plots for all traits are provided in Supplementary Materials (**Figures S2-S6**), while
228 illustrative plots for 15 focal traits are provided in the main text (**Figure 2**). Similarly,
229 phenotypic correlations within the BC1 population were examined among all traits
230 (**Table S3**), while relationships among a subset of focal traits are presented in the main
231 text (**Figure 3**). Given significant correlations among many of the floral morphological

232 traits and among color attributes (**Table S3**), we also used principle component analyses
233 (PCAs) to create separate composite metrics (principle components (PCs)) for three
234 groups of traits (i.e. Morph PC1-PC3; Nectar Color PC1-3; Petal Color PC1-PC3; **Table**
235 **S4**) as additional measures of floral variation. Trait correlations, including PCs, are
236 provided in **Table S5**, and distribution plots are provided in **Figures S3-S5**.

237 ***Genotyping and linkage map construction:*** Genomic DNA was extracted from
238 young leaf tissue from the 2 parental individuals, 13 F1s (including the F1 parent used to
239 generate the population), and 269 BC1s, using the Qiagen DNeasy Plant Mini Kit. DNA
240 quantity and quality were confirmed via Nanodrop (Fisher Scientific) and gel
241 electrophoresis with λ DNA-HindIII Digest marker (New England BioLabs). Samples
242 were then sent to Novogene Corporation (Beijing) for genotyping-by-sequencing (GBS).
243 GBS libraries were prepared using optimized restriction enzymes (MseI and HaeIII), and
244 following insert size selection, sequenced on an Illumina Hi-Seq to generate 150bp paired
245 end reads. Raw reads were trimmed and filtered using Trimmomatic (Bolger et al. 2014),
246 and read quality was checked pre- and post-trimming using fastqc (Andrews 2010). To
247 identify SNPs, cleaned reads were mapped to the domesticated tomato genome (Tomato
248 Genome Consortium 2012) using the mem function in BWA (Li 2013). Alignment files
249 were then input into the STACKS refmap pipeline (Catchen et al. 2013) to determine
250 genotypes. Reads and genotype data are available in NCBI SRA XXXXXX.

251 To construct the linkage map, we first removed markers that were genotyped in
252 less than 35% of individuals, or showed significant segregation distortion (i.e. alleles at
253 >80% or <20% frequency). The linkage map was constructed using the MST and
254 Kosambi algorithms, implemented in the R package ASMap (Taylor and Butler 2017).

To alleviate map expansion issues, we removed markers which consistently differed from neighboring markers in terms of genotype assignment, indicating a high likelihood of genotyping error. The linkage map was then finalized using the ripple function in R package R/qtl (Broman et al. 2003).

Identifying QTL: We implemented Haley-Knott regression in R/qtl to identify QTL contributing to each trait. To account for potential environmental contributions to trait variation, we included date of measurement (Month) and location within the greenhouse (Bench) as covariates in our QTL scans. Putative QTL were first identified using the scanone function, followed by permutations for genome-wide LOD significance thresholds. Two dimensional scans (scantwo function) were used in the stepwise qtl function to fit multiple QTL models. These models were used to identify significant QTL, their 1.5 LOD confidence intervals, their effect sizes (i.e. difference in phenotype mean between homozygotes and heterozygotes), and the total amount of phenotypic variance explained by each QTL, as well as interactions among QTL, and potential contributions of covariates. QTL were considered to be co-localized if their 1.5 LOD intervals overlapped. Significant co-localization was assessed by comparing overlap among identified QTL to overlap from 10000 randomly generated distributions, for traits within each category (morphological, color/physiological, or fertility), and between each trait category. Briefly, a custom Python script was used to generate random distributions of QTL (by randomly re-distributing the identified QTL among the 12 linkage groups), and the observed frequency of co-localization in each was recorded for each randomization to generated count distributions, in R. All code used to generate the linkage map, identify QTL, and assess QTL co-location, is available on GitHub

278 (https://github.com/gibsonMatt/jaltomataQTL).

279

280 **RESULTS**

281 ***Segregation patterns suggest additive alleles underlie most traits***

282 Most traits were significantly different between the two parental species (**Table**
283 **1**). F1 means were intermediate for most traits as well, except that petals were generally
284 brighter (more white) than either parent (**Figures S5+S7**). Other than fruit set and seed
285 germination rates, all traits were unimodally distributed within the BC1s; phenotypic
286 values were intermediate between F1s and the recurrent parent (*J. sinuosa*) for many of
287 these traits, consistent with additive effects (**Figure 2; Figures S2-S6**). Several traits (7
288 of 25) showed transgressive segregation within the BC1s, including some floral
289 morphological traits, nectar volume and color, and seed viability and germination rates
290 (**Table S2; Figures S2-S6**).

291

292 ***Significant correlations observed within – but generally not between – floral***
293 ***morphology, floral color, and fertility trait categories***

294 Within the BC1s, most trait combinations were not strongly associated.
295 Nonetheless, several correlations remained significant following multiple testing
296 (Bonferroni) correction (**Table S3**), primarily associations that are expected biologically,
297 including allometric relationships among floral organs and positive associations among
298 related fertility traits. For instance, corolla diameter was significantly positively
299 associated with most other morphological traits, suggesting shared genetic control of
300 overall floral size (**Figure 3**), while corolla diameter was also significantly negatively

301 correlated with proportion of corolla fusion (i.e. shorter corolla tubes had wider limbs and
302 longer tubes had narrower limbs, r = -0.348, $p = 8.68e^{-8}$). These relationships were
303 recovered with PCA on morphology traits, in which PC1-PC3 explained 76% of the
304 variance among BC1s (**Table S4**). Based on trait loadings, PC1 corresponds to floral
305 width vs. depth, PC2 to overall floral size, and PC3 to relative reproductive organ
306 dimensions. Similarly, related fertility traits also remained strongly correlated, such as
307 fruit mass with seed set, and number of viable pollen grains with proportion of viable
308 pollen (**Table S3**). Finally, color attributes within each of nectar color and petal color
309 were strongly correlated with one another, but these attributes were not associated
310 between nectar and petals (**Table S3**). From PCAs on nectar color and petal color
311 attributes (separately), PC1-PC3 for each explained 97% and 94% of the variance among
312 BC1s, respectively (**Table S4**).

313 In contrast, there were relatively few significant correlations among different trait
314 categories. Notable exceptions, however, included a positive relationship between floral
315 size and nectar volume as well as floral size and certain aspects of nectar color (**Figure 3;**
316 **Table S3**). There were also significant positive correlations between pollen viability and
317 each of several components of flower size (as well as Morph PC2 or "size") (**Tables**
318 **S3+S5**). This latter relationship seems to be explained by anther size: across 15 *Jaltomata*
319 species, mean viable pollen count is significantly associated with anther size prior to
320 dehiscence ($F = 15.56$, $p = 0.0017$) (J.L. Kostyun, unpub.).

321

322 ***Linkage map construction recovered 12 linkage groups***

323 Mapping high quality reads to the tomato genome identified 25,136 SNPs that

324 differentiated the two parental species. Following all subsequent filtering (removing
325 markers genotyped in less than 35% of individuals, with high segregation distortion or
326 non-Mendelian inheritance, or with high likelihood of genotyping errors), we retained
327 520 high quality markers. Linkage map construction recovered 12 linkage groups (LGs),
328 which correspond to the number of chromosomes in the parental species (Mione et al.
329 1993; Chiarini et al. 2017). Based on orthology with tomato, we were able to confidently
330 assign 5 of these LGs to chromosomes (**Figure 4**). Total map length was 1593.71 cM
331 (65.17 cM – 324.48 cM per chromosome/LG), with an average of 2.92 cM between
332 markers (**Figure 4**).
333
334 ***Few moderate-effect QTL underlie most traits, with little QTL co-localization between***
335 ***trait categories***
336 We identified a total of 63 QTL for our 25 traits (with 4 additional loci for PC
337 traits). Most traits had 2-4 QTL, with a range of 0-6 QTL (**Table 2**, **Table S6**). Alleles at
338 55 of 67 QTL (82%) acted in the direction consistent with parental values (i.e. the allele
339 from paternal donor *J. umbellata* moved the phenotype of BC1s closer to its species
340 mean) (**Table 2**), and the amount of phenotypic variation explained per QTL ranged from
341 2-28%. The latter range suggests that we had reasonable power to identify QTL with
342 even relatively small effects--explaining as little as 2% of the variance. Consistent with
343 observed trait segregation patterns, significant interactions among QTL within individual
344 traits were identified in few cases: for ovary diameter and certain nectar color attributes
345 (**Table 2**, **Table S6**).
346 Although every linkage group had at least one QTL, QTL were not distributed

347 uniformly across the genome, with notable clusters on LG1 and LG9 (**Figure 4, Table 2**).
348 We also identified several instances of QTL co-localization within trait categories,
349 especially for morphology and fertility traits, which each had significantly more cases of
350 co-localization (1.5 LOD overlap) than expected by chance (133 observed vs. upper
351 bound of 115 expected overlaps, $p = 7.5e^{-4}$; 8 observed vs. upper bound of 4 expected
352 overlaps, $p = 7.0e^{-6}$, respectively) (**Table S7; Figure S8**). These co-localization instances
353 included QTL for biologically-related traits (e.g. petal length and corolla diameter, or
354 fruit mass and seed set; **Table S6**), for which we already observed strong correlations
355 (**Table S3**). In some cases, co-localized QTL share the same or a very close peak marker
356 (e.g. petal length, corolla fusion, and ovary diameter on LG12; **Table S6**) which is
357 suggestive of potential pleiotropy, however we note that the large 1.5 LOD intervals of
358 some QTL will increase instances of incidental co-localization events.

359 In contrast, co-localization between different trait categories was never greater
360 than expected by chance, with co-localization between morphology and color traits
361 actually significantly less than expected ($p = 0.016$) (**Table S7; Figure S8**). This is
362 consistent with mostly incidental occurrences of overlap between QTL for traits in
363 different categories. Nonetheless, we did detect co-localized QTL at the same or very
364 close peak markers for, for example, nectar color (RGB) and volume on LG3 (**Figure 4;**
365 **Table S6**) and for nectar color (a), corolla fusion, and corolla depth on LG7, (**Table S6**),
366 which provide intriguing cases of potential adaptive pleiotropy (i.e. alleles at QTL that
367 simultaneously act to increase floral size, nectar darkness, and/or nectar volume).
368

369 **DISCUSSION**

370 Genetic correlations among different components of the phenotype, especially
371 resulting from pleiotropy, can constrain or facilitate trait evolution (Agrawal and
372 Stinchcombe 2009). Pleiotropy could have particularly strong effects on the evolution of
373 traits that are functionally integrated, such as those comprising the flower (Armbruster et
374 al. 2009; Smith 2016). To better understand the genetic architecture underlying floral trait
375 evolution within florally diverse *Jaltomata*, including whether pleiotropy might have
376 shaped observed variation, we examined patterns of genetic segregation and genetic
377 architecture for 25 floral and fertility traits in a hybrid (BC1) population between species
378 with highly divergent floral traits. We found that most of our examined traits have a
379 relatively simple genetic basis, with few to moderate QTL with largely additive effects.
380 We also identified strong correlations and significant QTL overlap within trait categories,
381 but few associations across different types of traits. The exceptions however, between
382 certain aspects of floral morphology and nectar traits, are consistent with existing trait
383 associations that are observed across the genus, suggesting that these could be examples
384 of adaptive pleiotropy. Overall, our data suggest that the rapid floral trait evolution
385 observed in this group could have been facilitated by a relatively simple genetic basis for
386 individual floral traits, and a general absence of antagonistic pleiotropy among different
387 types of reproductive traits, especially morphology and color.
388
389 ***Few genetic changes could underlie floral trait shifts***
390 The relatively simple genetic architecture that we detect for most of our floral
391 traits might be one mechanism that has permitted rapid floral evolution within the genus.
392 Indeed, our inference that few QTL controlling corolla traits agrees with comparative

393 development data from these species (Kostyun et al. 2017) in which we observe that
394 relatively simple heterochronic changes in corolla trait growth rates distinguish these
395 rotate vs. tubular corolla forms. Interestingly, our findings are also consistent with
396 previous studies of floral trait genetics between closely related species (Smith 2016). For
397 instance, one or few QTL have been found for species differences in nectar volume in
398 several other systems (e.g. Bradshaw et al. 1998; Stuurman et al. 2004; Wessinger et al.
399 2014; but see Nakazato et al. 2013), similar to our inference of a single QTL for this trait.
400 For petal and nectar color, we identified 2 and 5 QTL, respectively, each with moderate
401 to major effects (**Table 2, Table S6**), similar to other systems that generally identify few
402 loci of large effect for petal color (e.g. Bradshaw et al. 1998; Wessinger et al. 2014).
403 Perhaps unlike these cases, however, it is likely that loci controlling color differences in
404 *Jaltomata* are regulators of pigment quantity rather than presence/absence biosynthesis,
405 because both nectar and petal color show gradation in the BC1s rather than discrete color
406 bins. Moreover, preliminary data from a VIGS (virus-induced gene silencing) pilot study
407 in *J. sinuosa* indicate that the purple petal pigment is an anthocyanin (J.L. Kostyun and
408 J.C. Preston, unpub.), whereas for nectar color, preliminary data suggest that an indole-
409 flavin contributes to red pigment in *J. umbellata* (J.L. Kostyun and D. Haak, unpub.),
410 consistent with our inference that color variation is unassociated between these different
411 floral components.

412 In addition to relatively few contributing loci, many of the examined traits also
413 appear to be underpinned by additive effects (**Table 1; Figure 3; Figures S2-6**), while
414 epistatic effects were comparatively rare. Both are factors that might also facilitate more
415 rapid responses to selection. Other studies have similarly found that floral size traits are

416 often additive (Gottlieb 1984). Although several floral traits showed transgressive
417 segregation within our BC1s, which could indicate epistatic interactions, similar patterns
418 can result from unique combinations of additive alleles that have opposite effects in the
419 parental species (e.g. deVicente and Tanksley 1993) and we identified individual QTL
420 with these opposing effects for many of these traits. In comparison, significant interaction
421 effects among morphological QTL were detected for ovary diameter only (**Table 2**),
422 consistent with a general lack of epistatic interactions for this class of traits.

423 The notable exceptions to additivity involved many of the fertility traits (as well
424 as some components of color, see below). BC1 individuals tended to have lower seed set
425 and poorer quality seeds (decreased viability and response to germination-inducing
426 stimuli), and the recombinant BC population contained a subset of highly sterile
427 individuals. The segregation of recombinant individuals with reduced viability and
428 fertility often occurs in hybrids (Baack et al. 2015), including in hybrids from additional
429 *Jaltomata* species pairs (Kostyun and Moyle 2017). Such patterns are typically due to
430 deleterious epistatic interactions between loci that have diverged between the two
431 parental lineages, as has been shown in close relatives including tomatoes (Moyle and
432 Nakazato 2008; Sherman et al. 2014). These observations in *Jaltomata* are similarly
433 consistent with a specific role for epistasis among incompatible alleles in the expression
434 of postzygotic reproductive isolation.

435

436 ***Reduced constraints may also have facilitated rapid floral trait evolution***

437 Because rapid floral evolution may occur either through a lack of antagonistic
438 pleiotropy or through adaptive pleiotropy, we assessed evidence for these potential

439 mechanisms within *Jaltomata*. Within trait categories, we detected positive but modest
440 associations between several floral size traits, and among biologically related fertility
441 traits (e.g. fruit size and seed set) (**Figure 3; Table S3**), as well as significant co-
442 localization of QTL for these groups of traits (**Table S7**). Morphological associations in
443 particular suggest that shared growth regulators (e.g. Sicard and Lenhard 2011; Brock et
444 al. 2012) contribute to - but do not completely determine - observed variation in floral
445 organ sizes. In contrast, we detected fewer instances of strong trait correlations and QTL
446 co-localization between different trait categories (**Table S3**, **Table S7**). This general lack
447 of antagonistic pleiotropy among different classes of floral and fertility traits may have
448 facilitated rapid floral evolution in this system by minimizing constraints on the available
449 combinations of floral traits. Despite this general pattern, we did identify several
450 instances of QTL co-localization that might represent adaptive pleiotropy. Most notably,
451 larger flowers generally produced darker (more red) nectar as well as a greater volume of
452 nectar, as reflected in co-localization of QTL underlying aspects of floral morphology
453 and both nectar volume and color (**Table 2; Figure 4; Table S6**). Interestingly, this trait
454 combination (large flowers with copious dark nectar) is actually not exhibited by either
455 parental species used in this experiment (**Figure 1; Table 1**); however, it is found in
456 numerous other *Jaltomata* species (see below; Miller et al. 2011; Kostyun and Moyle
457 2017) and is consistent with recognized pollination syndromes (e.g. Fenster et al. 2004).
458

459 ***Ecological context for rapid floral change in* Jaltomata**

460 Overall, our findings suggest potential mechanistic explanations for the evolution
461 of remarkable floral trait diversity among *Jaltomata* species within the last 5 million

462 years (Sarkinen et al. 2013). Traits with a relatively simple genetic basis that are
463 uncoupled from other floral and fertility traits have fewer mechanistic constraints, and
464 therefore can more rapidly respond to selective opportunities as they arise. Although we
465 have not yet directly assessed the role of selection in shaping floral differences among
466 species, several features of *Jaltomata* floral biology are consistent with pollinator-
467 mediated selection on floral traits (van der Niet and Johnson 2012), likely in conjunction
468 with mating-system related changes (Goodwillie et al. 2010). First, floral trait variation
469 within *Jaltomata* shows clear hallmarks of selection imposed by pollinator
470 differentiation. Nearly all species in the earliest diverging *Jaltomata* lineage have
471 relatively small, ancestrally rotate flowers with small amounts of lightly colored nectar,
472 and hymenopterans have been observed visiting several of these species (T. Mione, pers.
473 comm.). In contrast, many species in the South American derived clade—including *J.*
474 *umbellata* examined here--have attractive features associated with vertebrate pollination
475 (Fenster et al. 2004). Several of these are visited by hummingbirds (T. Mione, per.
476 comm.), notably those with larger flowers with a highly fused corolla (either campanulate
477 or tubular) and copious amounts of darkly colored nectar; intriguingly, this repeated
478 natural trait covariation is consistent with the genetic association between floral size and
479 nectar traits we identified here.

480 These features indicate that pollinators are a likely source of selection for floral
481 differentiation among species within *Jaltomata*, but they do not necessarily explain why
482 *Jaltomata* as a genus has been uniquely responsive to this pollinator variation, especially
483 in comparison to its most close relatives. Species from both *Solanum* and *Capsicum* are
484 found within the same geographical regions as *Jaltomata*, and are therefore exposed to

485 the same pollinator variation, but are nonetheless almost uniformly rotate and bee-
486 pollinated (Knapp 2010). Interestingly, one important difference between *Jaltomata* and
487 these two genera is in their predominant mating system. Self-incompatibility is the
488 ancestral state in the Solanaceae (Steinbachs and Holsinger 2002) and is broadly
489 persistent in both *Solanum* and *Capsicum* (Goldberg et al. 2010). In contrast, all
490 examined *Jaltomata* species are self-compatible (Mione 1992; J.L. Kostyun and T.
491 Mione, unpub.), indicating that gametophytic self-incompatibility was lost early in the
492 evolution of this clade. Moreover, the presence of delayed selfing and strong herkogamy
493 in many species (e.g. Mione et al. 2015; Mione et al. *in review*), in addition to field
494 observations of pollinators (above; T. Mione, pers. comm.), indicate that species most
495 likely employ a mixed mating strategy in their native ranges. The absence of genetically-
496 determined self-incompatibility and the predominance of mixed mating strategies might
497 have uniquely facilitated the evolution of new floral trait variation in *Jaltomata*,
498 compared to either *Capsicum* or *Solanum*. Mixed mating strategies are generally
499 observed to maintain the largest amount of floral trait variation, compared to predominant
500 selfing or enforced outcrossing (Goodwillie et al. 2005; Rosas-Guerrero et al. 2014). In
501 addition, they have been predicted to facilitate pollinator shifts--especially to pollinators
502 that might be more efficient but potentially unreliable (such as hummingbirds)—because
503 they allow reproductive assurance (via selfing, when pollinators are limited) and increase
504 the expression of new floral trait variation controlled by recessive alleles (Goodwillie et
505 al. 2005; Brys et al. 2013; Wessinger and Kelly 2018). Notably, our data indicate that
506 dark/red colored nectar is at least partially recessive (**Figure 2**), and that red petal
507 pigmentation is completely recessive (**Figure S7**), consistent with this novel variation

being based on new recessive alleles.

CONCLUSIONS

Genetic correlations among floral traits, especially those due to pleiotropic effects, likely shape permitted trajectories of floral evolution. To assess how such genetic associations might have contributed to observed patterns of floral diversity in *Jaltomata*, we examined segregation patterns and genetic architecture of 25 floral and fertility traits in a hybrid (BC1) population generated from parents with divergent floral traits. Our data are consistent with several mechanisms that could have allowed rapid floral trait evolution in this system: a largely simple genetic basis underlying variation in most of our floral traits, a general absence of antagonistic pleiotropy constraining floral evolution, and a potential instance of adaptive pleiotropy governing floral size and nectar traits. This genetic architecture, in combination with pollinator-mediated selection on a background of self-compatible mixed mating, might have uniquely positioned this genus for the rapid floral diversification now evident within *Jaltomata*.

ACKNOWLEDGEMENTS

We thank the IU greenhouse staff for plant care, CJ Jewell and David Haak for logistical support, undergraduate research assistants (especially Meret Thomas-Huebner, Devki Shukla, and Shachia Jackson) for assistance with data collection, and Tim Leslie for assistance with simulations. This work was supported by the IU Biology Department, National Science Foundation Award (NSF DEB 1136707) to LCM, and National Science Foundation Graduate Research Fellowship Program (NSF DEB 1342962) and Doctoral

Dissertation Improvement Grant (NSF DEB 1601078) to JLK.

AUTHOR CONTRIBUTIONS

JLK and LCM designed the experiment, JLK generated experimental materials, JLK and CMK collected phenotypic data, JLK and MJSG analyzed the data, and JLK and LCM wrote the paper with input from CMK and MJSG.

REFERENCES

Agrawal, A. F., and J. R. Stinchcombe. 2009. How much do genetic covariances alter the rate of adaptation? *Proc R Soc Lond Biol* **276**:1183-1191.

Andrews, S. 2010. FastQC: a quality control tool for high throughput sequence data. Available online at: http://www.bioinformatics.babraham.ac.uk/projects/fastqc

Armbruster, W. S., T. F. Hansen, C. Pelabon, R. Perez-Barrales, and J. Maad. 2009. The adaptive accuracy of flowers: measurement and microevolutionary patterns. *Ann Bot* **103**:1529-1545.

Armbruster, W. S., C. Pelabon, G. H. Bolstad, and T. F. Hansen. 2014. Integrated phenotypes: understanding trait covariation in plants and animals. *Proc R Soc Lond Biol* **369**.

Baack, E., M. C. Melo, L. H. Rieseberg, and D. Ortiz-Barrientos. 2015. The origins of reproductive isolation in plants. *New Phytol* **207**:968-984.

Bartlett, M. E. 2017. Changing MADS-Box Transcription Factor Protein–Protein Interactions as a Mechanism for Generating Floral Morphological Diversity. *Integrative and Comparative Biology* **57**:1312-1321.

554 Bradshaw, H. D., K. G. Otto, B. E. Frewen, J. K. McKay, and D. W. Schemske. 1998.
555 Quantitative trait loci affecting differences in floral morphology between two
556 species of monkeyflower (*Mimulus*). *Genetics* **149**:367-382.
557 Brock, M. T., P. X. Kover, and C. Weinig. 2012. Natural variation in GA1 associates
558 with floral morphology in *Arabidopsis thaliana*. *New Phytol* **195**:58-70.
559 Broman, K. W., H. Wu, S. Sen, and G. A. Churchill. 2003. R/qtl: QTL mapping in
560 experimental crosses. *Bioinformatics* 19:889-890.
561 Brys, R., B. Geens, T. Beeckman, and H. Jacquemyn. 2013. Differences in dichogamy
562 and herkogamy contribute to higher selfing in contrasting environments in the
563 annual *Blackstonia perfoliata* (Gentianaceae). *Ann Bot* **111**:651-661.
564 Bolger, A. M., M. Lohse, and B. Usadel. 2014. Trimmomatic: A flexible trimmer for
565 Illumina Sequence Data. *Bioinformatics*, btu170.
566 Catchen, J., P. A. Hohenlohe, S. Bassham, A. Amores, and W. A. Cresko. 2013. Stacks:
567 an analysis tool set for population genomics. *Mol Ecol* 22: 3124-3140.
568 Chiarini, F. E., D. Lipari, G. E. Barboza, and S. Knapp. 2017. In: IAPT/IOPB
569 chromosome data 25. K. Marhold and J. Kuccera (eds). *Taxon* 66: 1246–1252.
570 Conner, J. K. 2002. Genetic mechanisms of floral trait correlations in a natural
571 population. *Nature* **420**:407-410.
572 Conner, J. K., I. A. Cooper, R. J. La Rosa, S. G. Perez, and A. M. Royer. 2014. Patterns
573 of phenotypic correlations among morphological traits across plants and animals.
574 *Phil. Trans. R. Soc. B* **369**.
575 deVicente, M. C., and S. D. Tanksley. 1993. QTL analysis of transgressive segregation in
576 an interspecific tomato cross. *Genetics* **134**:585-596.

577 Ettensohn, C. A. 2013. Encoding anatomy: Developmental gene regulatory networks and
578 morphogenesis. *Genesis* **51**:383-409.
579 Farooq, M., S. M. A. Basra, N. Ahmad, and K. Hafeez. 2005. Thermal hardening: A new
580 seed vigor enhancement tool in rice. *J Integr Plant Biol* **47**:187-193.
581 Fenster, C. B., W. S. Armbruster, P. Wilson, M. R. Dudash, and J. D. Thomson. 2004.
582 Pollination syndromes and floral specialization. *Annu Rev Ecol Evol Syst* **35**:375-
583 403.
584 Garcia, J. E., A. D. Greentree, M. Shrestha, A. Dorin, and A. G. Dyer. 2014. Flower
585 Colours through the Lens: Quantitative Measurement with Visible and Ultraviolet
586 Digital Photography. *Plos One* **9**.
587 Goldberg, E. E., J. R. Kohn, R. Lande, K. A. Robertson, S. A. Smith, and B. Igic. 2010.
588 Species selection maintains self-Incompatibility. *Science* **330**:493-495.
589 Goodwillie, C., S. Kalisz, and C. G. Eckert. 2005. The evolutionary enigma of mixed
590 mating systems in plants: Occurrence, theoretical explanations, and empirical
591 evidence. *Annu Rev Ecol Evol Syst* **36**:47-79.
592 Goodwillie, C., R. D. Sargent, C. G. Eckert, E. Elle, M. A. Geber, M. O. Johnston, S.
593 Kalisz, D. A. Moeller, R. H. Ree, M. Vallejo-Marin, and A. A. Winn. 2010.
594 Correlated evolution of mating system and floral display traits in flowering plants
595 and its implications for the distribution of mating system variation. *New Phytol*
596 **185**:311-321.
597 Gottlieb, L. D. 1984. Genetics and morphological evolution in plants. *Am Nat* **123**:681-
598 709.
599 Hermann, K., U. Klahre, M. Moser, H. Sheehan, T. Mandel, and C. Kuhlemeier. 2013.

600 Tight Genetic Linkage of Prezygotic Barrier Loci Creates a Multifunctional
601 Speciation Island in *Petunia*. *Current Biology* **23**:873-877.
602 Jewell, C., A. D. Papineau, R. Freyre, and L. C. Moyle. 2012. Patterns of reproductive
603 isolation in *Nolana* (chilean bellflower). *Evolution* **66**:2628-2636.
604 Kendal, D., C. E. Hauser, G. E. Garrard, S. Jellinek, K. M. Giljohann, and J. L. Moore.
605 2013. Quantifying Plant Colour and Colour Difference as Perceived by Humans
606 Using Digital Images. *Plos One* **8**.
607 Knapp. S. 2010. On 'various contrivances': pollination, phylogeny and flower form in the
608 Solanaceae. *Phil Trans R Soc B* 365:449-460.
609 Kostyun, J. L. and L. C. Moyle. 2017. Multiple strong postmating and intrinsic
610 postzygotic reproductive barriers isolate florally diverse species of *Jaltomata*
611 (Solanaceae). *Evolution* **71**:1556-1571.
612 Kostyun, J. L., J. C. Preston, and L. C. Moyle. 2017. Heterochronic developmental shifts
613 underlie floral diversity within *Jaltomata* (Solanaceae). *EvoDevo* 8(1): 17.
614 Li, H. 2013. Aligning sequence reads, clone sequences and assembly contigs with BWA-
615 MEM. arXiv:1303.3997v1 [q-bio.GN].
616 Manceau, M., V. S. Domingues, R. Mallarino, and H. E. Hoekstra. 2011. The
617 Developmental Role of Agouti in Color Pattern Evolution. *Science* **331**:1062-
618 1065.
619 Miller, R. J., T. Mione, H. L. Phan, and R. G. Olmstead. 2011. Color by Numbers:
620 Nuclear Gene Phylogeny of *Jaltomata* (Solanaceae), Sister Genus to *Solanum*,
621 Supports Three Clades Differing in Fruit Color. *Syst Botany* **36**:153-162.

Mione, T. 1992. *The systematics and evolution of* Jaltomata *(Solanaceae)*. PhD Dissertation, The University of Connecticut. Available from ProQuest Dissertations & Theses Global. (303964972).

Mione, T., G. J. Anderson, and M. Nee. 1993. *Jaltomata* I: Circumscription, description and new combinations for five South American species. *Brittonia* 45: 138-145.

Mione, T., S. Leiva González, and L. Yacher 2015. Two new Peruvian species of *Jaltomata* (Solanaceae, Solaneae) with red floral nectar. *Brittonia* **67**:105-112.

Mione, T., K. C. Plourd, S. Leiva González, L. Yacher, C. T. Philbrick, and D. Blume. 2017. Pollination decreases longevity of the protogynous flowers of *Jaltomata sinuosa* (Solanaceae). *J Biol Nat* **7**:123–9.

Mione, T., J. L. Kostyun, and S. Leiva Gonzalez. In Revision. Self-compatibility, protogyny and locating the floral nectary of *Jaltomata quipuscoae* (Solanaceae).

Moyle, L. C., and T. Nakazato. 2008. Comparative genetics of hybrid incompatibility: Sterility in two Solanum species crosses. *Genetics* **179**:1437-1453.

Nakazato, T., L. H. Rieseberg, and T. E. Wood. 2013. The genetic basis of speciation in the Giliopsis lineage of Ipomopsis (Polemoniaceae). *Heredity* **111**:227-237.

Olmstead, R. G., L. Bohs, H. A. Migid, E. Santiago-Valentin, V. F. Garcia, and S. M. Collier. 2008. A molecular phylogeny of the Solanaceae. *Taxon* **57**:1159-1181.

Preston, J. C., L. C. Hileman, and P. Cubas. 2011. Reduce, reuse, and recycle: developmental evolution of trait diversification. *Am. J. Bot.* **98**:397-403.

RAW Therapee Team. 2012. Raw Therapee: cross-platform raw image processing program. http://rawtherapee.com/.

Rijpkema A, T Gerats, and M. Vandenbussche. 2006. Genetics of floral development in

645 Petunia. Pages 237-278 *in* L. J. Soltis DE, Soltis PS & Callow JA, editor. Adv Bot
646 Res: Incorp Adv Plant Pathol: Developmental Genetics of the Flower.
647 Rosas-Guerrero, V., R. Aguilar, S. Marten-Rodriguez, L. Ashworth, M. Lopezaraiza-
648 Mikel, J. M. Bastida, and M. Quesada. 2014. A quantitative review of pollination
649 syndromes: do floral traits predict effective pollinators? *Ecol. Lett* **17**:388-400.
650 Sarkinen, T., L. Bohs, R. G. Olmstead, and S. Knapp. 2013. A phylogenetic framework
651 for evolutionary study of the nightshades (Solanaceae): a dated 1000-tip tree.
652 *BMC Evolutionary Biology* **13**.
653 Schneider, C. A., W. S. Rasband, and K. W. Eliceiri. 2012. NIH Image to ImageJ: 25
654 years of image analysis. *Nature Methods* **9**:671-675.
655 Schwartzwald, D. 2012. Color Space Converter Plugin for ImageJ.
656 https://imagej.nih.gov/ij/plugins/color-space-converter.html.
657 Sherman, N. A., A. Victorine, R. J. Wang, and L. C. Moyle. 2014. Interspecific Tests of
658 Allelism Reveal the Evolutionary Timing and Pattern of Accumulation of
659 Reproductive Isolation Mutations. *Plos Genetics* **10**.
660 Shrestha, R., J. Gomez-Ariza, V. Brambilla, and F. Fornara. 2014. Molecular control of
661 seasonal flowering in rice, arabidopsis and temperate cereals. *Ann Bot* **114**:1445-
662 1458.
663 Sicard, A., and M. Lenhard. 2011. The selfing syndrome: a model for studying the
664 genetic and evolutionary basis of morphological adaptation in plants. *Ann Bot*
665 **107**:1433-1443.
666 Smaczniak, C., R. G. H. Immink, G. C. Angenent, and K. Kaufmann. 2012.
667 Developmental and evolutionary diversity of plant MADS-domain factors:

668 insights from recent studies. *Development* **139**:3081-3098.

669 Smith, S. D. 2016. Pleiotropy and the evolution of floral integration. *New Phytol* **209**:80-
670 85.

671 Stebbins, G.L. 1974. Flowering plants: evolution above the species level. Harvard
672 University Press, Cambridge, MA.

673 Steinbachs J.E., and K.E. Holsinger 2002. S-RNase-mediated gametophytic self
674 incompatibility is ancestral in eudicots. *Mol Biol Evol* **19**: 825–829.

675 Stuurman, J., M. E. Hoballah, L. Broger, J. Moore, C. Basten, and C. Kuhlemeier. 2004.
676 Dissection of floral pollination syndromes in *Petunia*. *Genetics* **168**:1585-1599.

677 Taylor, J., and D. Butler. 2017. R Package ASMap: Efficient Genetic Linkage Map
678 Construction and Diagnosis. *Journal of Statistical Software* 79:1-29.

679 Tomato Genome Consortium, The. 2012. The tomato genome sequence provides insights
680 into fleshy fruit evolution. *Nature* 485:635-641.

681 van der Niet, T., and S. D. Johnson. 2012. Phylogenetic evidence for pollinator-driven
682 diversification of angiosperms. *Trends Ecol Evolut* **27**:353-361.

683 Wagner, G. P., and J. Z. Zhang. 2011. The pleiotropic structure of the genotype-
684 phenotype map: the evolvability of complex organisms. *Nature Reviews Genetics*
685 **12**:204-213.

686 Wessinger, C. A., L. C. Hileman, and M. D. Rausher. 2014. Identification of major
687 quantitative trait loci underlying floral pollination syndrome divergence in
688 *Penstemon*. *Phil. Trans. R. Soc. B* **369**.

689 Wessinger, C. A., C. C. Freeman, M. E. Mort, M. D. Rausher, and L. C. Hileman. 2016.
690 Multiplexed shotgun genotyping resolves species relationships within the North

American genus *Penstemon*. *Am J Bot* **103**:912-922.

Wessinger, C. A., and J. K. Kelly. 2018. Selfing can facilitate transitions between pollination syndromes. *Am Nat* 191.

Wu, M., J. L. Kostyun, M. W. Hahn, and L. C. Moyle. 2018. Dissecting the basis of novel trait evolution in a radiation with widespread phylogenetic discordance. *Mol Ecol* 27: 3301-3316.

Wu, M., J. L. Kostyun, and L. C. Moyle. 2019. Genome sequence of *Jaltomata* addresses rapid reproductive trait evolution and enhances comparative genomics in the hyper-diverse Solanaceae. *Genome Biology and Evolution* in press. Available at: https://www.biorxiv.org/content/early/2018/05/30/335117.

Xu, S. Q., and P. M. Schluter. 2015. Modeling the two-locus architecture of divergent pollinator adaptation: how variation in SAD paralogs affects fitness and evolutionary divergence in sexually deceptive orchids. *Ecology and Evolution* **5**:493-502.

714 **Table 1**. Summary of measured floral and fertility traits within parental species, F1s, and
715 BC1s. Phenotypic means and variances provided, while significant differences between
716 parental species were assessed with t-tests on transformed data as appropriate (see
717 Methods). Note that significant differences in seed germination rates could not be tested.
718 * p<0.05, ** p<0.001; *** p<0.0001.

Trait	*J. sinuosa* (n=7)		*J. umbellata* (n=5)	
Floral Morphology/Physiology	**Mean**	**Variance**	**Mean**	**Variance**
Buds per Inflorescence	*2.86***	0.03	*8.60***	3.24
Calyx Diameter (mm)	*15.49***	0.08	*8.14***	2.91
Sepal Length (mm)	*7.48***	0.02	*4.41***	0.56
Corolla Diameter (mm)	*29.82****	1.92	*15.32****	5.70
Corolla Depth (mm)	*1.38***	0.07	*10.25***	5.52
Corolla Fusion (mm)	9.45	0.11	10.33	1.55
Corolla Fusion Proportion	*0.63**	0.001	*0.72**	0.001
Petal Length (mm)	14.85	0.41	14.40	0.16
Stamen Length (mm)	10.80	0.29	10.45	0.22
Anther Length (mm)	*2.03**	0.02	*1.73**	0.04
Ovary Diameter (mm)	*2.28****	0.03	*1.37****	0.05
Style Length (mm)	*7.90****	0.17	*14.64****	1.72
Herkogamy (mm)	*-2.20****	0.01	*5.37****	4.62
Nectar Volume (uL)	*6.86****	1.07	*17.80****	13.20
Floral Color				
Nectar Color - Intensity	*205.93****	144.59	*105.59****	106.17
Nectar Color - Red	207.88	222.00	219.47	274.81
Nectar Color - Green	*208.71***	148.02	*66.48***	239.95
Nectar Color - Blue	*201.35****	105.86	*30.79****	114.53
Nectar Color - Composite RGB	*-202.17****	115.02	*122.20****	48.24
Nectar Color - L	*83.49****	20.32	*50.42****	31.63
Nectar Color - a	*-1.55****	0.95	*57.61****	7.10
Nectar Color - b	*3.47****	8.20	*51.84****	59.31
Petal Color - Intensity	*137.05***	127.04	*112.33***	136.18
Petal Color - Red	135.85	138.57	128.59	114.35
Petal Color - Green	134.31	119.92	121.87	181.62
Petal Color - Blue	*140.97***	123.32	*86.55***	134.58
Petal Color - Composite RGB	*-139.42****	106.86	*-79.82****	208.17
Petal Color - L	83.18	2.59	84.15	4.86
Petal Color - a	*0.81**	0.02	*-0.93**	0.62
Petal Color - b	*-1.26****	0.02	*6.71****	1.05
Fertility				
Viable Pollen Grains	25143	36809254	26834	60773556
Proportion Viable Pollen	0.76	0.01	0.71	0.02
Fruit Set	*0.93**	0.01	*0.55**	0.06
Fruit Mass (g)	*0.47***	0.01	*0.12***	0.01
Fruit Diameter (cm)	*1.01**	0.01	*0.61**	0.02

Seed Set	*74.87**	256.92	*30.44**	494.43
Viable Seed Set	*74.87**	256.92	*23.59**	182.31
Viable Seed T50	9.33	--	7.00	--
Viable Seed MGT	22.00	--	14.00	--

Table 1 cont.

F1s (n=13)		BC1s (n=224)	
Mean	**Variance**	**Mean**	**Variance**
3.95	0.68	3.51	1.63
10.55	0.48	12.10	1.08
5.45	0.13	6.16	0.28
24.58	6.84	28.97	9.92
6.64	0.58	5.22	1.35
9.81	0.40	9.92	1.24
0.67	0.001	0.63	0.002
14.65	1.61	15.78	2.88
10.81	0.59	10.86	1.26
2.01	0.01	2.13	0.04
1.62	0.02	1.82	0.04
12.39	1.04	10.82	1.97
2.95	1.08	1.20	1.02
11.90	12.32	10.76	18.87
172.44	110.66	192.70	272.74
232.93	149.55	213.14	127.46
198.03	248.93	206.89	165.90
74.27	317.30	157.76	1591.28
-39.37	1182.31	-151.51	2429.74
81.31	14.35	83.99	13.42
-0.05	101.74	-4.29	14.91
59.85	75.94	22.91	287.97
147.02	63.03	135.30	119.75
152.60	100.19	137.00	144.35
154.91	246.30	135.92	138.89
137.41	105.01	132.70	113.98
-139.72	391.57	-131.62	142.13
86.93	5.82	83.56	4.60
-0.81	0.19	-0.04	0.36
2.89	3.13	0.75	1.29
22513	16602405	26886	145318716
0.82	0.00	0.74	0.03
0.93	0.01	0.89	0.03
0.24	0.01	0.29	0.01
0.80	0.01	0.85	0.03
36.06	168.37	37.67	361.12
25.46	303.95	26.28	340.08
34.00	1001.78	26.70	607.37
46.04	622.37	39.36	458.11

721 **Table 2**. Summary of identified QTL for key floral and fertility traits. Includes peak
722 location and LOD of QTL, 1.5 LOD intervals, amount of phenotypic variance of trait
723 explained, phenotypic effect size and standard error (back-transformed where applicable),
724 and whether the effect is aligned with parental trait values. Full QTL data, including the
725 full models for all traits, are provided in Table S6.

Trait Category	Trait	LG	Peak Location	Peak LOD
Flower Morph	Inflor. Size (2)	LG 4	55.4	3.04
		LG 1	56	3.02
	Calyx Dia (3)	LG 1	56	9.06
		LG 8	84.3	3.15
		LG 9	66	5.59
	Sepal Length (3)	LG 1	57	8.30
		LG 12	23	3.74
		LG 9	65.9	7.04
	Corolla Dia (3)	LG 4	21.1	3.50
		LG 12	37.4	1.57
		LG 8	73.1	5.87
	Corolla Depth (4)	LG 7	52	17.95
		LG 5	40.8	10.19
		LG 10	55.8	4.48
		LG 9	30	12.38
	Corolla Fusion Prop (4)	LG 5	86	3.57
		LG 4	26	3.77
		LG 1	72	4.60
		LG 9	16	7.19
	Petal Length (3)	LG 7	100	2.46
		LG 12	48.2	2.04
		LG 8	73	3.55
	Stamen Length (4)	LG 7	91	4.45
		LG 4	120.8	3.77
		LG 2	37.5	4.54
		LG 9	0	5.32
	Anther Length (1)	LG 1	18	3.78
	Ovary Dia (4)	LG 7	9.9	3.56
		LG 5	72	2.53

		LG 1	68	5.77
		LG 12	48.2	4.31
	Style Length (2)	LG 2	95.2	2.79
		LG 9	22	9.89
		LG 1	314	4.53
		LG 2	112	7.26
	Herkogamy (5)	LG 11	40	4.79
		LG 8	51.4	3.27
		LG 9	7.3	4.32
		LG 5	116	3.61
		LG 4	59.2	3.55
	PC1 (6)	LG 1	54.2	4.08
		LG 2	31.7	4.73
		LG 8	82	8.08
		LG 9	19	10.34
		LG 1	58	2.62
	PC2 (3)	LG 12	48.2	3.27
		LG 8	58	2.14
	PC3 (2)	LG 1	67.5	4.99
		LG 9	24.7	11.52
Flower Physio	Nectar Volume (1)	LG 3	187.2	2.81
		LG 7	28	9.91
	Nectar PC1 (3)	LG 5	100	13.15
		LG 2	153	5.48
	Nectar PC2 (1)	LG 7	8.4	3.29
Flower Color	Nectar PC3 (1)	LG 3	66.1	3.47
	Petal PC1 (1)	LG 5	65.3	5.83
	Petal PC2 (2)	LG 5	63	18.91
		LG 9	67	10.42
	Petal PC3 (0)	no QTL		
	Fruit Set (0)	no QTL		
	Fruit Dia (2)	LG 1	80	4.67
		LG 11	76.9	3.09
		LG 3	170	2.67
	Fruit Mass (4)	LG 1	96	5.47
Fertility		LG 11	76.5	5.63
		LG 12	0	4.51
	Seed Set (2)	LG 11	76	6.64
		LG 12	0	2.86
	Viable Seed Set (1)	LG 11	76.9	4.42
	Viable Pollen (0)	no QTL		

726

727 **Table 2 cont.**

1.5 LOD Intervals	%PVE	Effect	Effect SE	Aligned with Parental Value?
15-108	5.50	1.1576	0.0169	YES
34-133	5.46	-1.1628	0.0175	NO
49-81	13.67	-0.8026	0.1202	YES
69-92.55	4.46	-0.4565	0.1196	YES
17-85	8.13	-0.5976	0.1160	YES
49-70.73	12.17	-0.3923	0.0616	YES
10-59	5.22	-0.2539	0.0609	YES
22-73	10.18	-0.3404	0.0584	YES
13-70	4.47	1.3869	0.3440	NO
0-65.17	1.96	-0.9630	0.3606	YES
67-84	7.69	-1.9019	0.3596	YES
48-60.67	21.47	1.1455	0.1164	YES
20-46	11.20	0.8437	0.1187	YES
41-91	4.64	-0.5214	0.1140	NO
11-38	13.94	0.9420	0.1188	YES
80.21-99	5.39	0.0005	0.0000	YES
19-84	5.70	-0.0004	0.0000	NO
57-106	7.02	-0.0005	0.0000	NO
0-67	11.27	0.0008	0.0000	YES
25-100.67	3.29	1.0414	0.0050	NO
0-65.17	2.71	1.0390	0.0053	YES
39-92.55	4.78	-1.0657	0.0053	YES
59-100.67	5.68	0.5510	0.1209	NO
100-133	4.78	-0.4994	0.1194	YES
6-61	5.80	-0.5478	0.1190	YES
0-33	6.86	0.6194	0.1237	NO
8-35.87	6.48	-0.1157	0.0274	YES
0-25	5.56	-0.0936	0.0230	YES
0-84	3.90	0.0915	0.0269	NO
60-107	9.21	-0.1196	0.0229	YES
5-65.17	6.78	-0.1036	0.0231	YES
55-126	3.80	1.0517	0.0061	YES
1-30	14.51	1.1072	0.0063	YES
266-324	6.42	-1.1613	0.0141	NO
30-122	10.60	1.2156	0.0144	YES
5-63	6.81	1.2143	0.0783	YES
26-63	4.57	1.1344	0.0141	YES

3.47-32	6.12	1.1560	0.0140	YES
95-124.77	3.61	0.3880	0.1025	YES
24-76	3.55	-0.3691	0.0983	NO
34-86	4.08	0.3853	0.0958	YES
4-44	4.73	0.4121	0.0952	YES
68.51-92.55	8.08	0.5552	0.0981	YES
12-71	10.34	0.6040	0.0943	YES
43-138	3.72	-0.6666	0.1921	YES
16-62.42	4.69	-0.7556	0.1940	YES
36-92.55	3.03	-0.6066	0.1939	YES
46-86	7.27	-0.6665	0.1371	YES
20-31	18.01	-1.0720	0.1401	YES
172-187.19	5.22	1.2539	0.0366	YES
23-37	11.96	-1.5076	0.2152	YES
83-107	16.45	-1.9822	0.2413	YES
147-171.87	6.31	-1.1060	0.2174	YES
0-22	6.21	0.7061	0.1801	NO
17-121	6.92	-0.5691	0.1412	YES
60-72	11.4	-1.7713	0.3344	YES
59-67	28.06	-1.4839	0.1453	YES
39.15-73	14.09	-0.9231	0.1276	YES
61-103	8.64	-1.0608	0.0054	YES
51-79.93	5.61	-1.0463	0.0052	YES
48-187.19	4.07	-1.0168	0.0023	YES
60-146	8.58	-0.9745	0.0049	YES
54-79.93	8.85	-0.9762	0.0047	YES
0-10.64	7.01	-0.9771	0.0050	YES
63-79.93	12.28	-1.4353	0.0277	YES
0-63	5.07	-1.2857	0.0300	YES
68-79.93	8.85	-1.6267	0.0462	YES

734 **Figure Legends.**

735 **Figure 1**. Representative flowers of the parental species and their F1 hybrid.

736

737 **Figure 2**. Key trait distributions within the BC1 population, compared to phenotypic

738 means for *J. sinuosa* (purple line), *J. umbellata* (red line), and their F1s (pink line).

739

740 **Figure 3**. Key floral trait correlations within the BC1 mapping population. Scatterplots

741 are provided below the diagonal, while Spearman's correlation coefficients and

742 associated p-values are above the diagonal. Statistically significant correlations following

743 Bonferroni correction ($p < 3.125 \times 10^{-5}$) are highlighted in red. Correlation values for all

744 traits are provided in Table S3, and for PC traits provided in Table S5.

745

746 **Figure 4**. Linkage map and distribution of identified QTL (including 1.5 LOD intervals)

747 for 12 key floral and fertility traits.

748

749

750 **Supplementary Information**

751 **Table S1.** Accession information for material used and generated in this study.

752 **Table S2**. Trait measurements for all individuals phenotyped in this study.

753 **Table S3**. Correlations among all measured traits within BC1 individuals.

754 **Table S4**. Principle component loadings for highly correlated traits.

755 **Table S5**. Correlations among PC traits within BC1 individuals

756 **Table S6**. Full QTL models for all examined traits.

Table S7. Expected and observed counts of QTL overlap.

Figure S1. Measured morphological traits on mature flowers.

Figures S2-S3: Distributions for floral morphological and physiological traits within the mapping population.

Figure S4. Distributions for nectar color traits within the mapping population.

Figure S5. Distributions for petal color traits within the mapping population.

Figure S6. Distributions for fertility traits within the mapping population.

Figure S7. Representative examples of petal color variation among F1 individuals, compared to either parent.

Figure S8. Comparison of observed number of QTL overlaps with counts from 10000 randomly generated simulations, for QTL co-localization overlap within and between trait categories (morphology, color, and fertility).

J. sinuosa
F1
J. umbellata
1 cm

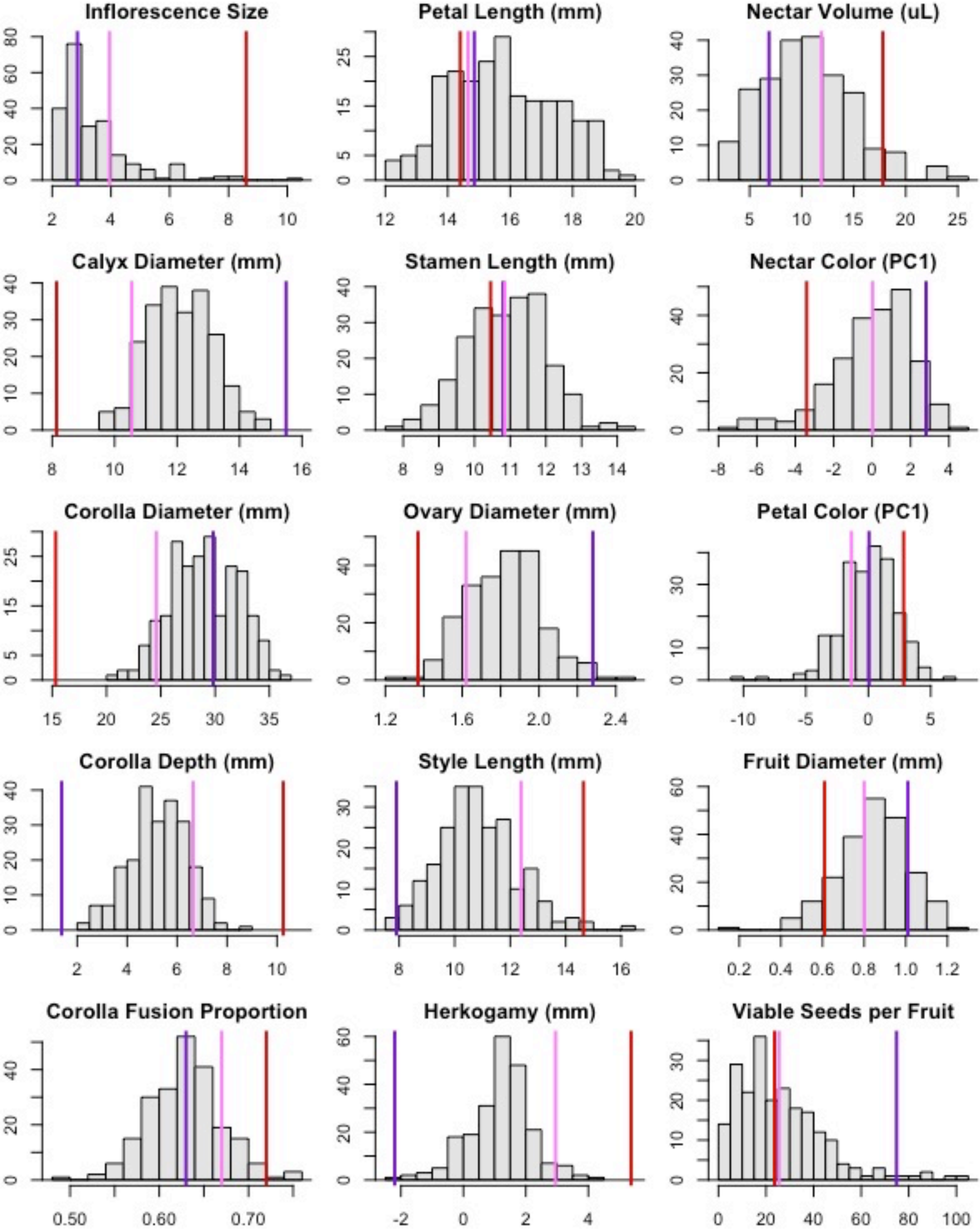
Inflorescence Size
Petal Length (mm)
Nectar Volume (uL)
Calyx Diameter (mm)
Stamen Length (mm)
Nectar Color (PC1)
Corolla Diameter (mm)
Ovary Diameter (mm)
Petal Color (PC1)
Corolla Depth (mm)
Style Length (mm)
Fruit Diameter (mm)
Corolla Fusion Proportion
Herkogamy (mm)
Viable Seeds per Fruit

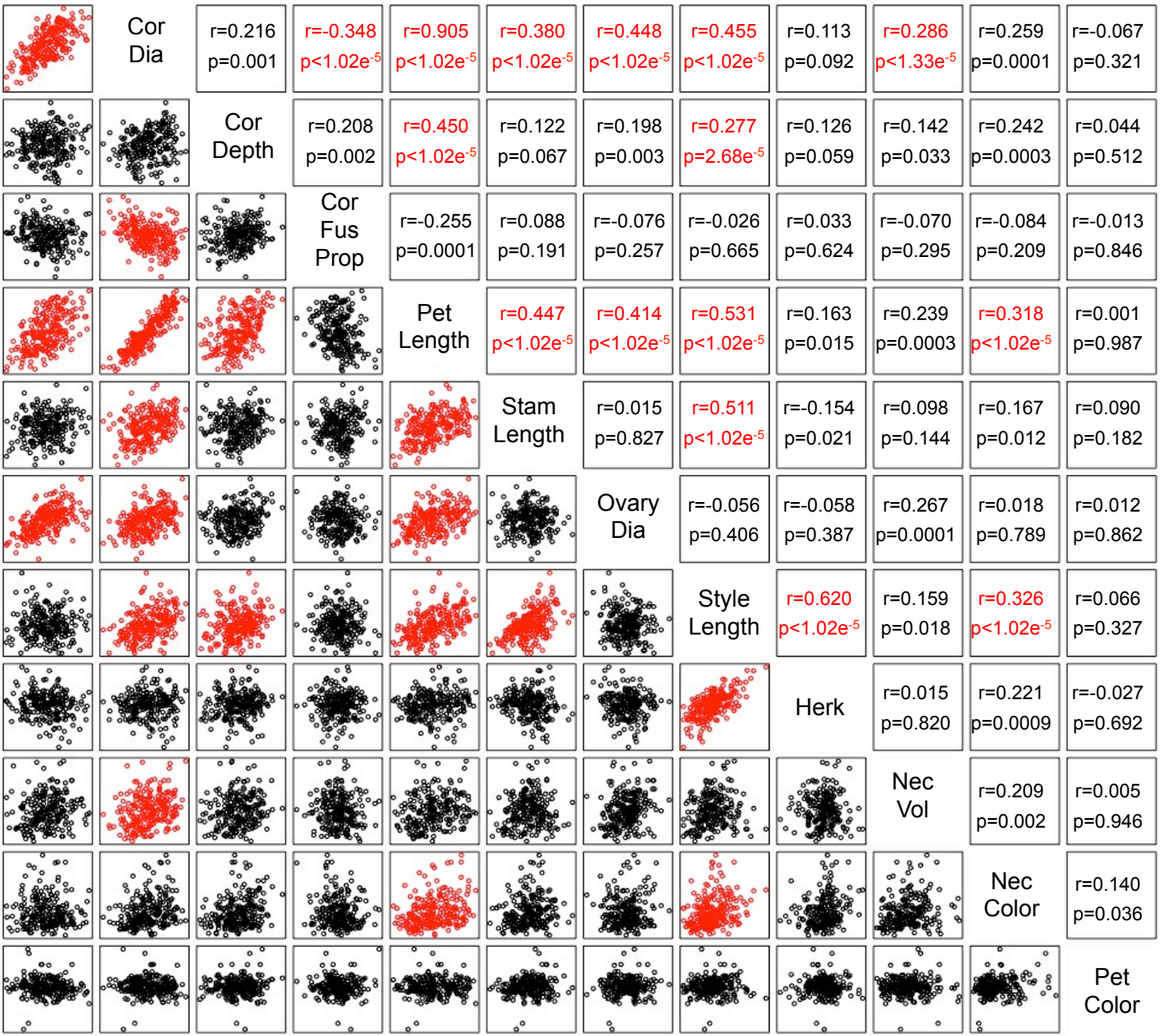

Calyx Dia	r=0.656 p<1.02e^{-5}	r=0.052 p=0.440	r=-0.162 p=0.015	r=0.548 p<1.02e^{-5}	r=0.105 p=0.118	r=0.571 p<1.02e^{-5}	r=0.001 p=0.989	r=-0.109 p=0.103	r=0.176 p=0.008	r=-0.040 p=0.551	r=-0.132 p=0.048
	Cor Dia	r=0.216 p=0.001	r=-0.348 p<1.02e^{-5}	r=0.905 p<1.02e^{-5}	r=0.380 p<1.02e^{-5}	r=0.448 p<1.02e^{-5}	r=0.455 p<1.02e^{-5}	r=0.113 p=0.092	r=0.286 p<1.33e^{-5}	r=0.259 p=0.0001	r=-0.067 p=0.321
		Cor Depth	r=0.208 p=0.002	r=0.450 p<1.02e^{-5}	r=0.122 p=0.067	r=0.198 p=0.003	r=0.277 p=2.68e^{-5}	r=0.126 p=0.059	r=0.142 p=0.033	r=0.242 p=0.0003	r=0.044 p=0.512
			Cor Fus Prop	r=-0.255 p=0.0001	r=0.088 p=0.191	r=-0.076 p=0.257	r=-0.026 p=0.665	r=0.033 p=0.624	r=-0.070 p=0.295	r=-0.084 p=0.209	r=-0.013 p=0.846
				Pet Length	r=0.447 p<1.02e^{-5}	r=0.414 p<1.02e^{-5}	r=0.531 p<1.02e^{-5}	r=0.163 p=0.015	r=0.239 p=0.0003	r=0.318 p<1.02e^{-5}	r=0.001 p=0.987
					Stam Length	r=0.015 p=0.827	r=0.511 p<1.02e^{-5}	r=-0.154 p=0.021	r=0.098 p=0.144	r=0.167 p=0.012	r=0.090 p=0.182
						Ovary Dia	r=-0.056 p=0.406	r=-0.058 p=0.387	r=0.267 p=0.0001	r=0.018 p=0.789	r=0.012 p=0.862
							Style Length	r=0.620 p<1.02e^{-5}	r=0.159 p=0.018	r=0.326 p<1.02e^{-5}	r=0.066 p=0.327
								Herk	r=0.015 p=0.820	r=0.221 p=0.0009	r=-0.027 p=0.692
									Nec Vol	r=0.209 p=0.002	r=0.005 p=0.946
										Nec Color	r=0.140 p=0.036
											Pet Color

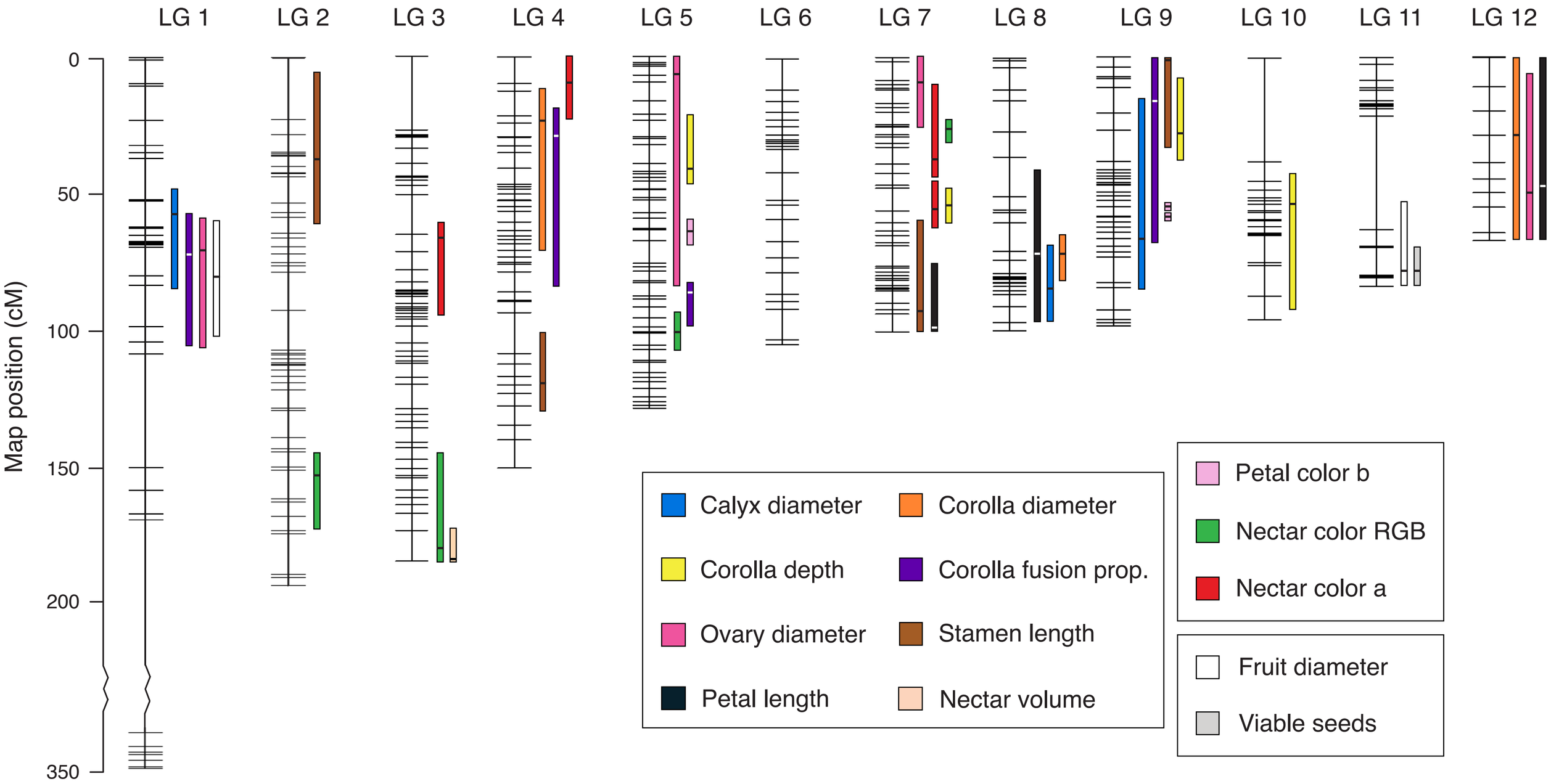
LG 1
LG 2
LG 3
LG 4
LG 5
LG 6
LG 7
LG 8
LG 9
LG 10
LG 11
LG 12
Map position (cM)
0
50
100
150
200
350
Calyx diameter
Corolla diameter
Corolla depth
Corolla fusion prop.
Ovary diameter
Stamen length
Petal length
Nectar volume
Petal color b
Nectar color RGB
Nectar color a
Fruit diameter
Viable seeds